

Detection of Moving Objects in Earth Observation Satellite Images: Verification

ERIC KETO¹ AND WESLEY ANDRÉS WATTERS²

¹*Harvard University, Institute for Theory and Computation
60 Garden Street, Cambridge, MA USA*

²*Wellesley College, Whitin Observatory
106 Central St., Wellesley, MA 02481, USA*

ABSTRACT

In multi-spectral images made by Earth observation satellites that use push-broom scanning, such as those operated by Planet Labs Corp., moving objects can be identified by the appearance of the object at a different locations in each spectral band. The apparent velocity can be measured if the relative acquisition time between images in different spectral bands is known to millisecond accuracy. The images in the Planet Labs archive are mosaics of individual exposures acquired at different times. Thus there is not a unique acquisition time for each spectral band. In an earlier paper, we proposed a method to determine the relative acquisition times from the information in the images themselves. High altitude balloons provide excellent targets to test our proposed method because of their high apparent velocity due to the orbital velocity of the satellite and geometric parallax in images aligned to the level of the ground. We use images of the Chinese balloon that crossed the US in February, 2024 as well as images of an identical balloon over Colombia to test our method. Our proposed method appears to be successful and allows the measurement of the apparent velocity of moving objects from the information available in the archive.

Keywords: METHODS: DATA ANALYSIS, TECHNIQUES: IMAGE PROCESSING.

1. INTRODUCTION

The satellites of Planet Labs Corp. (PLC) image most of the entire land area of the Earth with a daily revisit rate. The PLC archive of daily images extends back to 2020. While the satellites are not intended to provide motion detection as in a high frame-rate video, the arrangement of the filters to provide multi-spectral imaging in combination with the orbital motion of the satellite (push-broom scanning) provides a short video with the number of frames equal to the number of spectral bands. For example, in an RGB composite visual image, an object moving with sufficient apparent velocity appears as three individual objects with red, green, and blue colors. Images from PLC's most recent generation of satellites, named SuperDoves, show this effect in eight spectral bands and provide a video of an area equal the field of view with a duration equal to the time required for all spectral bands to cross the field of view, ~ 3.2 s duration. This allows a repurposing of the archived images to detect objects moving at speeds from about ten m^{-1} to several hundred m s^{-1} over most of the Earth during the times that the images were acquired, typically once per day around noon local time.

The analysis of the images to detect motion is trivial if the acquisition times of individual exposures are known. However, the images in the Planet Labs archive are mosaics of smaller area individual exposures and the acquisition times of the individual regions that make up the archived mosaic are not available in the archive. The mosaicing pattern is different for each composite image because the exposure or frame rate of the camera is asynchronous with the time required for the satellite to cross the field of view. Furthermore, the mosaicing algorithm as well as the details of the design of the satellites are considered proprietary technology by Planet Labs.

In an earlier article (Keto & Watters 2023), we proposed that it is nonetheless possible to determine enough information from the archived images to estimate the relative acquisition times between the different spectral bands in each region of the mosaic containing a moving object and then measure the velocities and altitudes of moving objects, subject to a well-known ambiguity between the velocity in a direction parallel to the orbital track of the satellite and

the altitude of the object. The principal assumption of our proposed method is that the camera on each satellite operates at fixed frame rate during the ~ 3.2 s time required to acquire enough images to make one mosaic.

In this article, we test this method using images of high-altitude balloons. High-altitude balloons are advantageous targets because the the motion of the balloon itself can be ignored in the analysis. The wind speed in the lower stratosphere, ~ 20 km altitude, is typically < 10 ms^{-1} (Limpinsel et al. 2018), and slow with respect to the apparent velocity due to parallax at altitude, ~ 300 ms^{-1} . Additionally, the balloons are incapable of significant acceleration within the ~ 3.2 s acquisition time that otherwise might confuse the analysis. We find the method successful. In the two examples studied, both with high signal-to-noise and high spatial resolution, we estimate errors less than 2% on the velocity and 3% on the altitude from the standard deviation of the individual measurements.

2. SELECTION OF TARGETS

There are numerous high altitude weather balloons that would serve as test objects. The passage of a large, high-altitude Chinese balloon across the continental US, February 3-6, provided an ideal target. The balloon is one of the larger high-altitude balloons, $\sim 40\text{m}$ versus ~ 6 m for a typical weather balloon. At ten times the resolution limit of the Planet Labs satellites, good positional accuracy is obtained with high signal-to-noise. Figure 1 shows the appearance of the Chinese balloon over British Columbia near the US-Canadian border in an image from satellite 2479. In addition, the publicity from the ensuing political antics played out in denials¹, accusations², and attempts at secrecy³ helped ensure that the balloon would be quickly located by Planet Labs with help from one of its partner companies, Synthetiaic. While searching, this collaboration also discovered a second balloon flying near Cartagena, Colombia on February 3, 2023 with characteristics identical to the Chinese balloon over the US.

We are grateful to Planet Labs for providing the scene identifications (table1) in the Planet Labs archives (private communication). From the available images, we selected the three made by the eight-band SuperDove satellites rather than the four-band Dove satellites because the former provide more positions for our analysis.

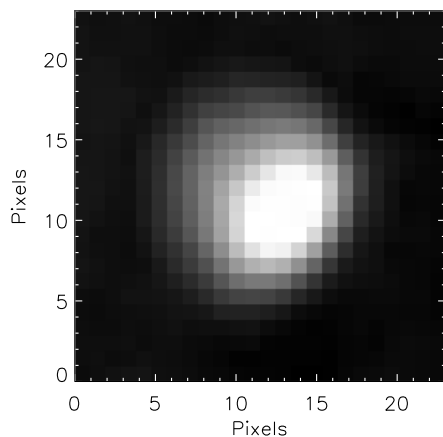


Figure 1. Image of a Chinese balloon over Columbia, near Cartagena, in visual blue, band 0, of the SuperDove satellite 247d. The pixel size is $(3 \text{ m})^2$.

¹ The airship is from China. It is a civilian airship used for research, mainly meteorological, purposes. Affected by the Westerlies and with limited self-steering capability, the airship deviated far from its planned course. The Chinese side regrets the unintended entry of the airship into US airspace due to force majeure. The Chinese side will continue communicating with the US side and properly handle this unexpected situation caused by force majeure. — Ministry of Foreign Affairs of the People’s Republic of China (Ministry of Foreign Affairs People’s Republic of China Feb 3, 2023)

² We were able to determine that China has a high-altitude balloon program for intelligence collection that’s connected to the People’s Liberation Army. — John Kirby, coordinator for strategic communications at the National Security Council (Vergun, D. Feb 13, 2023)

³ Reporter: Is the position of the balloon classified?

Pentagon Press Secretary Air Force Brig. Gen. Pat Ryder: What we’re not going to do is get into an hour-by-hour location of the balloon . . . right now it’s over the center of the continental United States. That’s about as specific as I’m going to get.

Reporter: Does the public not have a right to know if the balloon is over their state?

Ryder: The public certainly has the ability to look up in the sky and see where the balloon is. — from a press conference as reported by the WSJ Editorial Board (Feb 3, 2023)

Table 1. Planet Labs images with Chinese balloons

Approx. location	Scene ID	Satellite ID	Satellite Type
British Columbia	20230131_182637_88_2479	2479	8-band SuperDove
South Dakota	20230202_165236_51_242d	242d	4-band Dove
Missouri	20230203_161055_87_2439	2439	8-band SuperDove
South Carolina	20230204_151350_28_2458	2458	4-band Dove
South Carolina	20230204_154439_74_2495	2495	4-band Dove
Colombia	20230203_150645_50_247d	247d	8-band SuperDove

3. METHOD OF ANALYSIS

3.0.1. Locating the balloons

With their large size and high brightness, the balloons are easily located within the Planet Labs images by differencing pairs of the eight spectral bands in spectrally adjacent colors to show the balloon as a positive and negative pair at different positions against a suppressed background. We then use a template matching algorithm to locate the positions in each pair. Figures 2 and 3 show the locations of the balloons over Missouri and Colombia, respectively, in the eight spectral bands of satellites 2439 and 247d (table 1). The locations are shown over two backgrounds. The first is a 3-color visual image, and the second is an 8-band image formed from the sum of the absolute values of the differences of each pair of images.

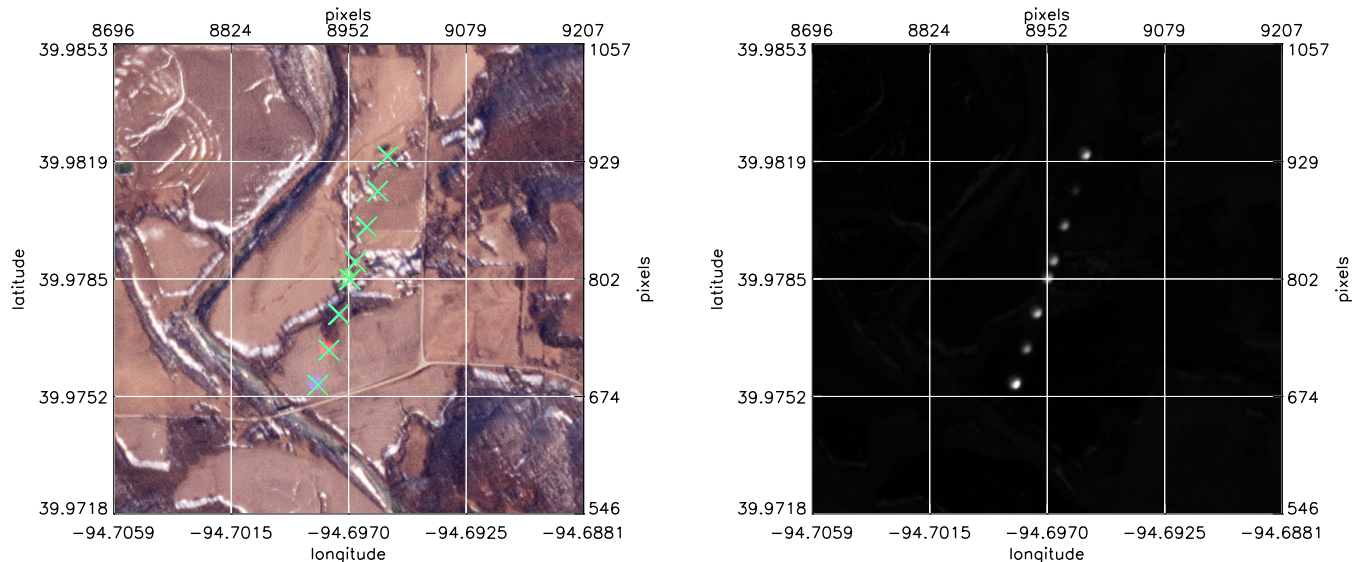


Figure 2. Positions of the first Chinese balloon over Missouri in the eight bands of SuperDove satellite 2439 against a 3-color visual background (*left*) and against the summed absolute values of the seven differenced pairs of images in the eight spectral bands (*right*). The bottom and left axes are labeled by longitude and latitude. The top and right axes shows the pixel coordinates with respect to the full images in the archive. On the visual image, the eight positions are marked by crosses. Only three images of the balloon appear in the red-green-blue visual representation. The balloon is seen in all eight spectral bands in the composite image of the summed differences (*right*). In the 8-band image (*right*), the balloon in the NIR band, second from the top in both figures, is not as bright because the sun is not as bright per unit wavelength in the NIR, and CCDs optimized for visible wavelengths generally have lower quantum efficiencies in the NIR.

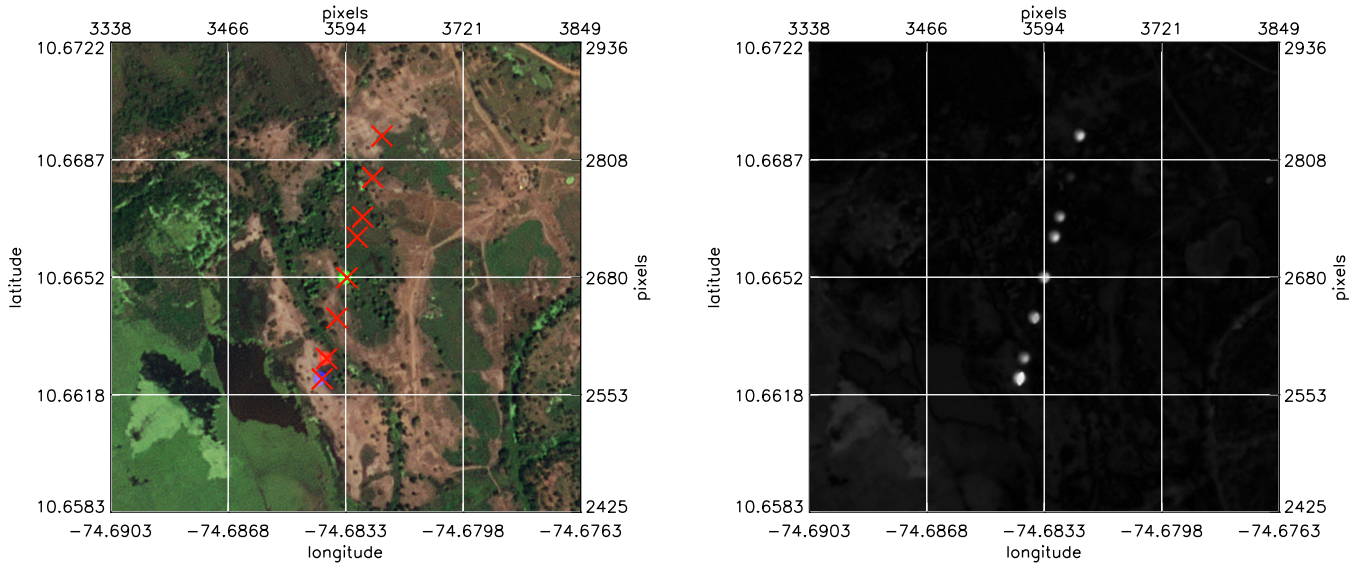


Figure 3. Positions of the second Chinese balloon over Colombia in the eight bands of SuperDove satellite 247d against a 3-color visual background (*left*) and against the summed absolute values of the seven differenced pairs of images in the eight spectral bands (*right*) in the format of figure 2.

3.1. Estimating the Relative Timing

Our method previously proposed to estimate the apparent velocity of an object in Planet Labs images is described in §4 of Keto & Watters (2023). The procedure has two steps. In the first step, we estimate the difference in the acquisition times of images in different spectral bands from the orbit of the satellite and the number of pixels on the sensor. In the second step, we determine the apparent velocity from the difference of positions of the balloon in each pair of spectral bands that are adjacent on the spectral filter and the relative acquisition times corrected for the mosaicing procedure that is used to combine several camera exposures into an archived image.

The first step is straightforward. From equation 1 of Keto & Watters (2023), the time difference between images of spectral bands whose individual filters are adjacent on the full filter is,

$$\Delta t_{color} = \frac{N_y \mu}{2\pi R_{\oplus} \omega}, \quad (1)$$

where the width in pixels of one color strip $N_y = 663$ is the total length/8 in pixels of the short side of the rectangular sensor array that is aligned with the direction of the satellite orbit, and the radius of the Earth, $R_{\oplus} = 6378$ km. The ground sample distance (GSD) or the length of a square pixel on the sensor projected on the surface of the Earth is $\mu \sim 4$ m. The exact GSD is returned in the search results of the Planet Labs archive. The mean motion, $\omega \sim 15.15$ orbits per day, is available from ephemerides published by Planet Labs with daily two-line element (TLE) models of the orbit of each satellite. The time difference between images of adjacent spectral bands is then $\Delta t_{color} \sim 0.39$ s.

The second step requires some educated guesswork about the proprietary and undisclosed design and operation of the satellites. The CCD sensor is preceded in the optical path by a filter with eight zones for the spectral bands. A single exposure of the camera produces an image conceptually similar to figure 4. For simplicity, figure 4 shows an image from satellite 247d in a single band, blue, whereas in the actual image, each of the horizontal zones is the image through one of the eight different spectral filters. The opaque red bars represent regions where the different filters are joined and the view through the filter is blocked. We consider the eight zones on the sensor to be divided by the horizontal midpoints of the red bars. The image has been rotated as if the satellite in a descending orbit were moving from north to south or vertically in the image.

The time required for the satellite to move the ground footprint of one sensor zone over the adjacent zone is ~ 0.39 s depending on the altitude of the satellite. Ignoring the obscured regions, if the camera frame rate were synchronized

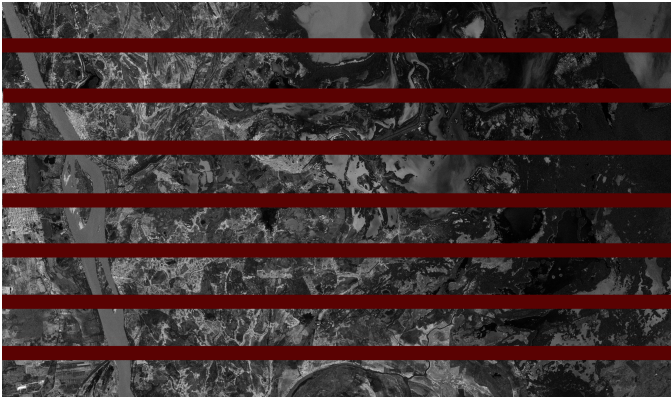


Figure 4. Mock-up of the image from a single exposure of the camera on a SuperDove satellite. The image is divided into eight zones, one for each spectral band. This mock-up shows the whole scene in a single band, blue, for simplicity whereas the images within the zones would be in different spectral bands. The red horizontal bars represent regions where the view is masked by the joints between the eight individual filters assembled together preceding the sensor. This representation is based on publicly available information and may not represent a single-frame image in detail.

with the rate, $\sim 1/0.39 = 2.56 \text{ s}^{-1}$, at which one zone moves over another (the color-crossing rate), a continuous mosaic in each of the colors could be constructed from eight exposures. However, to include the view of the ground below the blocked regions of the filter, the camera frame rate needs to be faster. Also the color-crossing rate is continuously increasing as the orbit of the satellite slowly decays. Since synchronization is not required to construct the mosaic, we assume that the camera frame rate is constant but asynchronous with the color-crossing rate. From an analysis of the images of the balloons, explained in the next section §3.2, we derive the camera frame rate as $\sim 1/0.18 = 5.55 \text{ s}^{-1}$, just faster than twice the color-crossing rate. Thus, the mosaic in a single spectral band of an image with as many pixels as the sensor is constructed from approximately 16 exposures of the camera. Importantly for our estimation of the apparent speed of an object, the difference in acquisition time between any two pixels of different colors is either the color-crossing time, 0.39 s, or the color-crossing time plus or minus the time between exposures 0.184 s (estimated in §3.2). The formula for the apparent velocity is then equation 2 of Keto & Watters (2023),

$$v_i = \frac{\Delta p}{\Delta t_{color} + a} \quad (2)$$

where $\Delta p = p_i(x, y) - p_{i+1}(x, y)$ is the distance between the locations of the object in two color bands, i and $i + 1$. The variable a can take one of three values: $0, \pm \Delta t_{camera}$. Equation 2 here is explained equivalently but differently in Keto & Watters (2023).

Analysis of the images from satellite 2479, discussed in §3.2 indicates that the mosaicing procedure is more complex than a simple translation of the full images to align with features on the ground. Refraction due to atmospheric turbulence may distort regions of the image that can be corrected in the mosaicing. Microscale turbulence on time scales of microseconds typically results in blurring on arc second scales, approximately the pixel size, and cannot be corrected by mosaicing. Less frequent mesocale turbulence with a longer spatial and time scale may shift the apparent position of ground features within an image. Since most of the visual distortion results from the denser atmosphere near the ground, the positional accuracy of objects at high altitude may be adversely affected by mosaicing corrections to align ground features. The significance of this effect and the circumstances in which it might apply are difficult to assess. The images from satellites 2439 and 247d do not appear to be affected.

3.2. Verification

We apply the proposed method to the images from satellites 2439 and 247d showing balloons over Missouri and Colombia, in figures 2 and 3, respectively. Both show equal displacements of the apparent position of the balloons in the different spectral bands with three exceptions. Figure 2 shows that the displacement between the image of the balloon in the center of the figure with respect to the adjacent image of the balloon just to the north is about half the length of the other displacements. Figure 3 shows two such occurrences at different places. This indicates that the value of a in equation 2 has a value of the negative of the time delay between camera exposures of the color bands at these locations in the image and zero elsewhere along the track of the balloon.

We can estimate the camera frame rate as follows. With the assumption that the balloon has no proper motion and therefore no acceleration, we expect equally spaced displacements between color bands except for the change caused by the time delay between exposures. The time delay between exposures is then found from equation 2 as the value that results in a constant velocity in the direction of the satellite orbit. The time delay between exposures is then 0.184 ± 0.007 s for both balloons and the average apparent velocities are 338 ± 5.0 and 371 ± 4.3 m/s. The errors on the apparent velocities are estimated empirically from the standard deviations of the measurements in table 2.

Table 2. Displacements and Apparent Velocities of Balloon Images Between Color Bands

2439		247d	
Segment	App. Vel.	Segment	App. Vel.
(m)	(m/s)	(m)	(m/s)
120	335	67	371
122	340	136	371
120	335	136	371
60	345	136	375
120	335	68	375
122	343	133	363
119	332	138	377

We can also estimate the altitude of a balloon from the ratio of the distance traveled by the satellite to distance traveled by the image of the balloon on the ground,

$$\frac{h_{sat} - h_{ball}}{h_{ball}} = \frac{L_{sat}}{L_{ground}} \quad (3)$$

We find altitudes of 21206 ± 341 m and 21505 ± 442 m for the first and second balloons over Missouri and Colombia respectively. The altitude of the first balloon at a different position, over South Dakota, was previously reported by Planet Labs as 20117 m (with no estimated error) as measured from an image taken by satellite 242d. (Xiao, M., Jhaveri, I., Lutz, E., Koetti, C., & Barnes, J.E. Mar 21, 2023). The difference in the two reported altitudes is within 3σ . It's also possible that the balloon was attempting to escape by fleeing to higher altitude during its eastward travel over the US. The altitude of the second balloon over Colombia has not previously been reported.

3.3. Loss of Ground Referencing over Snow and Ice

The first balloon was also spotted in an image made by SuperDove satellite 2479 while it was over British Columbia, Canada, before it crossed into the US. Figure 5 shows the apparent positions of the balloon in the same format as figures 2 and 3. The ground is completely covered with white snow and ice consistent with the winter conditions, and no features for ground reference that are required for positional accuracy are apparent. The only significant feature in any of the spectral bands is the balloon itself. The mosaicing algorithm applied by Planet Labs has evidently mistaken the exceptionally bright balloon for a ground reference feature and attempted to align the spectral images on the balloon itself. This results in physically impossible apparent locations for the balloon.

NOTE ADDED

This research is conducted as part of the Galileo Project at Harvard University whose goal is to collect scientific quality data that may be useful in the search for objects of extraterrestrial origin (<https://projects.iq.harvard.edu/galileo/home>).

ACKNOWLEDGMENTS

We acknowledge Planet Labs Corp. for access to the data and for technical support.

REFERENCES

- Keto, E., & Watters, W. 2023, *Journal of Astronomical Instrumentation*, 23, 234007
- Limpinsel, M., Kuo, D., & Vjih, A. 2018, in 2018 IEEE 7th World Conference on Photovoltaic Energy Conversion (WCPEC) (A Joint Conference of 45th IEEE PVSC, 28th PVSEC & 34th EU PVSEC), 3367–3373

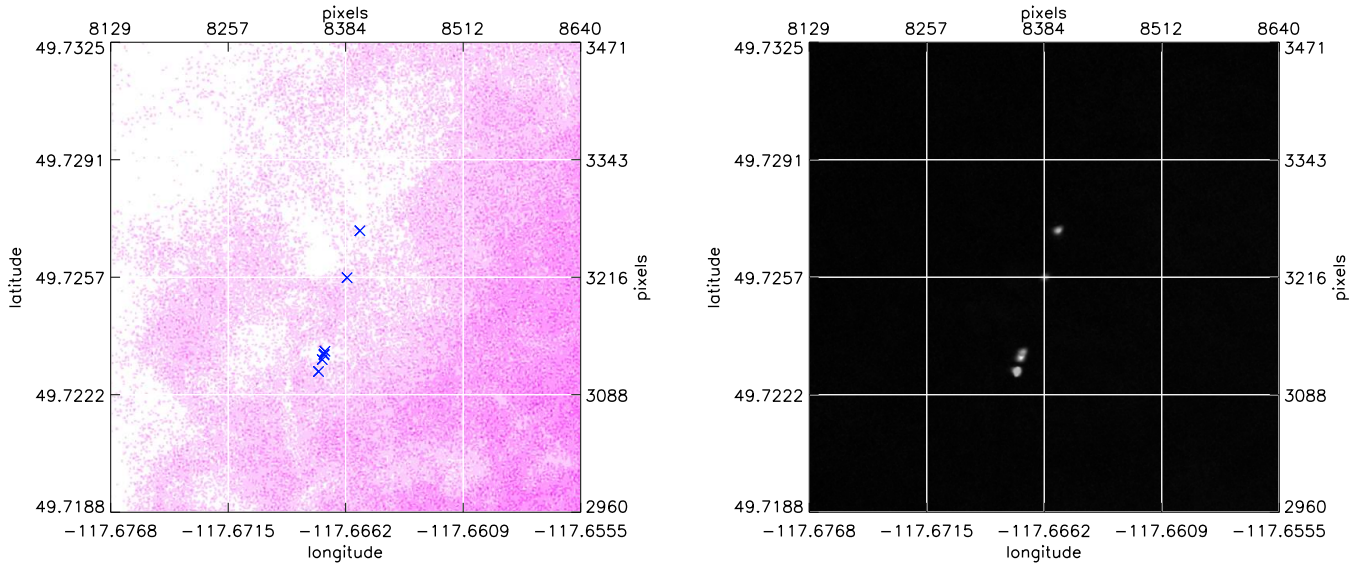


Figure 5. Positions of the first Chinese balloon over British Columbia in the eight bands of SuperDove satellite 2479 against a 3-color visual background (*left*) and against the summed absolute values of the seven differenced pairs of images in the eight spectral bands (*right*) in the format of figure 2. The pink color in the visual image in this image from satellite 2479 appears to be due to severe digital compression of the archived image. The actual scene should be all white.

Ministry of Foreign Affairs People's Republic of China. Feb 3, 2023, Foreign Ministry Spokesperson's Remarks on the Unintended Entry of a Chinese Unmanned Airship into US Airspace Due to Force Majeure, https://www.fmprc.gov.cn/mfa_eng/xwfw_665399/s2510_665401/202302/t20230203_11019484.htm, Ministry of Foreign Affairs People's Republic of China

Vergun, D. Feb 13, 2023, Chinese Surveillance Balloons Global in Scope, Says Official, <https://www.defense.gov/News/News-Stories/Article/Article/3297104/chinese-surveillance-balloons-global-in-scope-says-official>, New York Times

WSJ Editorial Board. Feb 3, 2023, Notable & Quotable: The Pentagon and the Wandering Chinese Balloon, <https://www.wsj.com/articles/notable-quotable-the-pentagon-wont-say-where-the-chinese-balloon-is-national-security-classified-11675453292>, The Wall Street Journal

Xiao, M., Jhaveri, I., Lutz, E., Koetti, C., & Barnes, J.E. Mar 21, 2023, Tracking the Chinese From Space, <https://nyti.ms/3naU7o8>, New York Times